IEEE Photonics Journal
An IEEE Photonics Society Publication

Open Access

All-Optical Arbitrary-Point Stable Quadruple Frequency Dissemination With Photonic Microwave Phase Conjugation

Volume 10, Number 4, August 2018

Haojie Wang
Xiaoxiao Xue
Shangyuan Li
Xiaoping Zheng

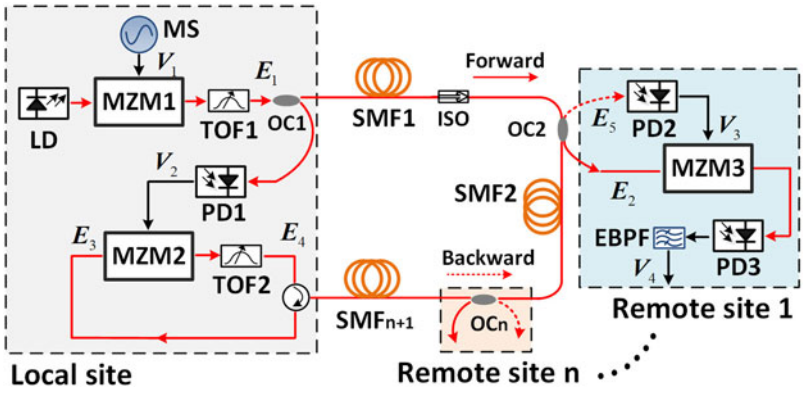

DOI: 10.1109/JPHOT.2018.2856515
1943-0655 © 2018 IEEE

All-Optical Arbitrary-Point Stable Quadruple Frequency Dissemination With Photonic Microwave Phase Conjugation

Haojie Wang, Xiaoxiao Xue, Shangyuan Li, and Xiaoping Zheng

Beijing National Research Center for Information Science and Technology, Department of Electronic Engineering, Tsinghua University, Beijing 100084, China

DOI:10.1109/JPHOT.2018.2856515

Manuscript received June 17, 2018; revised July 10, 2018; accepted July 12, 2018. Date of publication July 13, 2018; date of current version July 26, 2018. This work was supported in part by the National Nature Science Foundation of China (NSFC) under Grants 61690191, 61690192, 61420106003, and 61621064, in part by Beijing Natural Science Foundation under Grant 4172029, and in part by Chuanxin Funding. Corresponding author: Xiaoping Zheng (e-mail: xpzheng@mail.tsinghua.edu.cn).

Abstract: We present an all-optical stable quadruple frequency dissemination for an arbitrary-access-point fiber-optic loop link using photonic microwave phase conjugation. A two-tone optical carrier is transferred as a round-trip probe signal to undergo the propagation delay of the entire fiber loop link. When the probe signal returns to the local site, a Mach–Zehnder modulator biased at the null point is used as a phase conjugator to reverse its phase, thus, implementing photonic microwave phase conjugation. At an arbitrary remote site, the phase-conjugated signal is photomixed with a tapped forward transferred signal to obtain a stable frequency-quadrupled radio frequency (RF) signal in which the fiber-induced phase drift is automatically eliminated. Owing to photonic microwave phase conjugation and photomixing, the local oscillator leakage and harmonics interference of electrical mixers employed in the previous compensation schemes can be avoided. We demonstrate the stable dissemination of a 20-GHz frequency-quadrupled RF signal to two arbitrary remote sites located at a 20-km fiber-optic loop link. The residual root-mean-square timing jitter in an hour is no more than 0.86 ps. The relative frequency stability of 10^{-16} level at 1000 s averaging time can be realized at every remote site.

Index Terms: Frequency dissemination, fiber-optics loop links, passive phase correction, photonic microwave phase conjugation.

1. Introduction

Ultrastable radio-frequency (RF) dissemination has been an indispensable part of many advanced application systems such as particle accelerators, very-long-baseline interferometry (VLBI), comparison of optical clocks, and multi-telescope arrays [1], [2]. Compared to satellite links, fiber-optic links leveraging lower loss, larger bandwidth, higher reliability, and immunity to electromagnetic interference, are considered to be a promising option for stable and long-distance RF transfer [3]–[5]. Unfortunately, temperature variation as well as mechanical perturbation will introduce a propagation delay change of fiber-optic links, thus leading to the phase fluctuation of the transferred RF signals [6].

Active compensation scheme and passive compensation scheme have been proposed to cancel the fiber-induced phase drift and implement highly stable RF signal distribution [7]–[13]. Active compensation scheme generally utilizes the phase error from a round-trip probe signal to achieve the feedback control of a compensator. The compensators mainly include variable electrical delay lines [7], cylindrical piezoelectric transducers [8], tunable lasers [9], and phase locked loops [10], to name just a few. Although this scheme can accomplish very high phase stability, the response speed and phase recovery time are restricted by the compensation device's parameter. Passive compensation scheme based on frequency mixing has drawn extensive attention, since it can realize rapid and endless phase fluctuation compensation, and also get rid of complicated phase error detection and feedback circuits [11]–[13].

Recently, based on passive phase fluctuation compensation method, multi-node stable frequency dissemination schemes have been reported to underpin the applications, such as deep space network and distributed coherent aperture radar systems [14]–[18]. Such schemes are demonstrated over a branching or circular fiber-optic link. In the branching link, multi-wavelength techniques are used to discriminate among multi-access sites [16], [17]. As the number of access sites increases, the wavelength spacing between the local site and remote access sites will be extended. Consequently, the group velocity dispersion variation caused by temperature will be the inevitable limitation against the system performance improvement [16]. Moreover, the complexity and flexibility of the branching links need to be carefully considered due to the different configurations between the remote site and the access nodes. Based on the loop link, an arbitrary-access stable fiber delivery of RF signals has been proposed, where only one laser with a single wavelength is applied to mitigate temperature-induced group delay changes [18]. On the other hand, this scheme uses electrical mixers or multipliers to implement multistage frequency mixing, which can partly limit system performance at higher RF frequency such as millimeter-wave. In addition, these electronic components will bring about some local oscillator leakage and harmonics interference that can slightly degrade the precision of the phase stability [17].

In this paper, we propose and experimentally demonstrate an all-optical stable quadruple frequency dissemination scheme for an arbitrary-point fiber loop link using photonic microwave phase conjugation. A 20 GHz frequency-quadrupled RF signal is steadily disseminated along a 20-km fiber-optic loop link to an arbitrary remote site. The root-mean-square (RMS) timing jitter of the 20-GHz RF signal with photonic-microwave-phase-conjugation-based compensation is remarkably reduced from $\sim$180 ps to no more than 0.86 ps within an hour. The long-term frequency stability can reach 10^{-16} level at 1000 s averaging time. In this scheme, no auxiliary mixers or multipliers are required, so that the local oscillator leakage and nonlinear spurs can be circumvented. Furthermore, it provides a compact solution to highly stable millimeter-wave signal distribution with only one laser and simple optical components.

2. Topology and Operation Principle

The schematic diagram of the all-optical arbitrary-point stable quadruple frequency dissemination based on photonic microwave phase conjugation is illustrated in Fig. 1(a). The local site and remote site are connected via a fiber-optic loop link. If there are n remote sites, the fiber-optic loop link will consist of n + 1 single-mode fibers (SMFs). For simplicity, we just analyze the situation of one remote site, but meanwhile the corresponding operation principle is also applicable to any remote site with the same configuration. Here, we take the remote site 1 as an example. The principle of the proposed scheme can be understood as follows. At the local site, a two-tone optical carrier is generated by optical carrier-suppressed double-sideband (CS-DSB) modulation and optical filtering. The two-tone optical carrier is then split into two branches by an optical coupler (OC1). One branch is transmitted along the entire fiber loop link and back to the local site as a probe signal. The probe signal is modulated by the beat signal of the other branch, which can generate its phase-conjugated signal. Subsequently, the phase-conjugated signal is transmitted back to the remote site, and photomixed with a forward transferred signal to automatically eliminate the fiber-induced phase fluctuation and obtain a stable frequency-quadrupled RF signal.

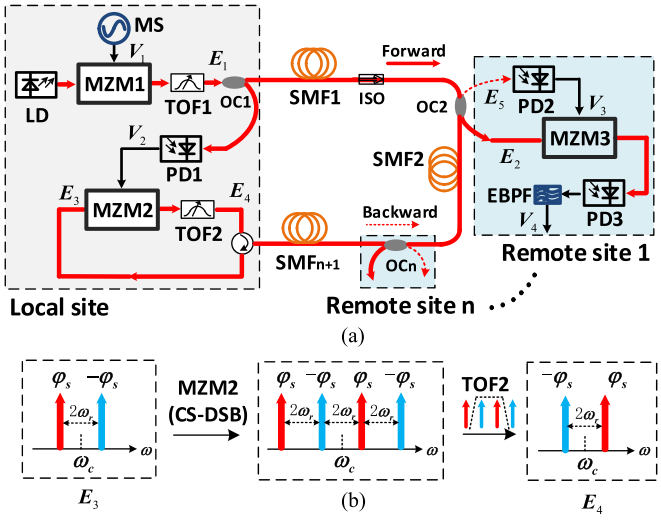

Fig. 1. (a) The schematic diagram of the proposed all-optical arbitrary-point dissemination of stabilized frequency-quadrupled RF signal over a fiber loop link. MS: microwave source. LD: laser diode. MZM: Mach-Zehnder modulator. TOF: tunable optical filter. PD: photodetector. OC: optical coupler. ISO: isolator. EBPF: electrical bandpass filter. SMF: single-mode fiber. (b) The spectrum evolution of the photonic microwave phase conjugation.

Here, we illustrate the proposed photonic microwave phase conjugation incorporating the spectrum evolution. At the local site, the standard RF signal generated by a microwave source (MS) can be denoted as:

$$V_1 = \cos(\omega_r t + \varphi_r), \tag{1}$$

where ω_r and φ_r represent its angular frequency and initial phase, respectively. Its amplitude is normalized for simplicity. V_1 modulates an optical carrier from a laser diode (LD) at the first Mach-Zehnder modulator (MZM1) biased at its null point for CS-DSB modulation. Considering an ideal situation of carrier suppression, the two first-order optical sidebands (OSBs) selected out by a tunable optical filter (TOF1) can be expressed as:

$$E_1 \propto \exp(i\omega_c t) \cdot \left\{\exp[-i(\omega_r t + \varphi_r)] + \exp[i(\omega_r t + \varphi_r)]\right\}, \tag{2}$$

where ω_c is the angular frequency of the optical carrier; and the initial phase is assumed to zero. The two first-order OSBs constitute the desired two-tone optical carrier. Then, E_1 is divided into two branches. One branch is detected by a photodetector (PD1) to obtain a frequency-doubled RF signal that is written as:

$$V_2 \propto \cos[2(\omega_r t + \varphi_r)]. \tag{3}$$

At the other branch, the two-tone optical carrier is firstly transferred over SMF1 to the remote site 1, where the 2 × 2 OC2 couples out a forward transferred optical signal that can be written as:

$$E_2 \propto \exp[i\omega_c(t - \tau_1)] \cdot \left\{\exp[-i(\omega_r t - \varphi_1 + \varphi_r)] + \exp[i(\omega_r t - \varphi_1 + \varphi_r)]\right\}, \tag{4}$$

where $\varphi_1 = \omega_r \tau_1$ indicates the accumulated phase change corresponding to the propagation delay τ_1 of SMF1. The other part is injected into SMF2 and returns to the local site as a round-trip probe signal. At the local site, the round-trip probe signal E_3 can be expressed as:

$$E_3 \propto \exp[i\omega_c(t - \tau_s)] \cdot \left\{\exp[-i(\omega_r t - \varphi_s + \varphi_r)] + \exp[i(\omega_r t - \varphi_s + \varphi_r)]\right\}, \tag{5}$$

where $\tau_s = \tau_1 + \tau_2$ is the propagation delay of the entire fiber link, and $\varphi_s = \omega_r \tau_s = \varphi_1 + \varphi_2$ is the corresponding phase change. $\varphi_2 = \omega_r \tau_2$ denotes the phase change of SMF2 with propagation delay τ_2. If n remote sites are connected to the fiber-optic loop link, $\varphi_s = \varphi_1 + \varphi_2 + \cdots + \varphi_k + \cdots + \varphi_n$

where $\varphi_k = \omega_r \tau_k$, $k = 1, 2, \ldots n$ is the phase fluctuation of the kth segment of SMF with propagation delay τ_k. Next, E_3 is modulated by the frequency-doubled RF signal V_2 at MZM2. Likewise, MZM2 is operated at the null point for CS-DSB modulation. The spectrum evolution of the modulation procedure is clearly shown in Fig. 1(b). The upper (blue) and lower (red) optical carrier of the probe signal E_3 are imposed with the fiber-induced phase fluctuation φ_s and $-\varphi_s$, respectively. Ignoring the high-order OSBs, four first-order OSBs are generated after ideal CS-DSB modulation at MZM2. Since the frequency spacing of the two optical carriers of the probe signal E_3 is $2\omega_r$ equal to the frequency of the modulated electrical signal V_2, the two first-order OSBs in the middle realize phase exchange. After that, the two first-order OSBs are filtered out by TOF2, and the output optical signal is expressed as

$$E_4 \propto \exp[i\omega_c(t-\tau_s)] \cdot \left\{\exp[-i(\omega_r t + \varphi_s + \varphi_r)] + \exp[i(\omega_r t + \varphi_s + \varphi_r)]\right\}. \tag{6}$$

Note that, the RF signal carried on E_4 (i.e., the terms in the curly braces) is a conjugate signal relative to that on E_3 in term of φ_s. Hence, photonic microwave phase conjugation is attained, and no electrical mixers or auxiliary microwave sources are needed.

The phase-conjugated signal E_4 is propagated backward to the remote site along SMF2. Owing to much slower fiber-delay vibration, the forward and backward signals transmitted over SMF2 would undergo the same propagation delay [11]. Consequently, E_5 which is extracted from the backward signal by OC2 can be written as:

$$\begin{aligned} E_5 &\propto \exp[i\omega_c(t-\tau_2-\tau_s)] \cdot \left\{\exp[-i(\omega_r t - \varphi_2 + \varphi_s + \varphi_r)] + \exp[i(\omega_r t - \varphi_2 + \varphi_s + \varphi_r)]\right\} \\ &= \exp[i\omega_c(t-\tau_2-\tau_s)] \cdot \left\{\exp[-i(\omega_r t + \varphi_1 + \varphi_r)] + \exp[i(\omega_r t + \varphi_1 + \varphi_r)]\right\}. \end{aligned} \tag{7}$$

After photodetection by PD2, the phase-conjugated RF signal is

$$V_3 \propto \cos[2(\omega_r t + \varphi_1 + \varphi_r)]. \tag{8}$$

At MZM3 biased at a quadrature point, V_3 modulates the trapped forward transferred signal E_2 that carries a RF signal with frequency of $2\omega_r$ and the fiber-induced phase fluctuation of $-2\varphi_1$. After photomixing at PD3, the phase $2\varphi_1$ of V_3 and $-2\varphi_1$ of the electrical signal carried by E_2 are exactly counteracted. Therefore, the term of sum frequency in the mixing product is filtered out by an electrical bandpass filter (EBPF) and expressed as

$$V_4 \propto \cos\,[4(\omega_r t + \varphi_r)], \tag{9}$$

the frequency and phase of which are fourfold that of the standard RF signal V_1. Furthermore, the phase fluctuation caused by fiber links has been automatically removed. Due to no mixers and multipliers in this scheme, undesired spurious signal can be circumvented, and an all-optical stable quadruple frequency dissemination is implemented.

3. Experiment and Discussion

The experiment setup of the proposed scheme is shown in Fig. 2. To evaluate the dissemination performance conveniently, the local site and an arbitrary remote site are located at the same place, which is in our laboratory. They are connected by a 20-km fiber loop link, consisting of two 10-km SMF spools jointed by OC2. The couple ratio of OC2 is 50:50. At the local site, a 5-GHz standard RF signal is generated by a Vector Signal Generator (Agilent E8267D), which is used to modulate an optical carrier from the LD (Keysight 81606A). The wavelength and output power of the optical carrier are 1552.24 nm and 16 dBm, respectively. For MZM1 we use a 10 Gb/s intensity modulator which is biased at V_p. In our experiment, MZM2 is substituted with a single-drive dual-parallel MZM (SD-DPMZM, Fujitsu FTM7961EX) to attain a higher carrier suppression ratio [19]. Additionally, we adjust carefully the central frequency and bandwidth of two TOFs at the local site to minimize the interference of high-order OSBs and acquire a two-tone optical signal. PD1 with a bandwidth of 12 GHz beats the forward two-tone optical signal and a narrowband EBPF centered at 10 GHz

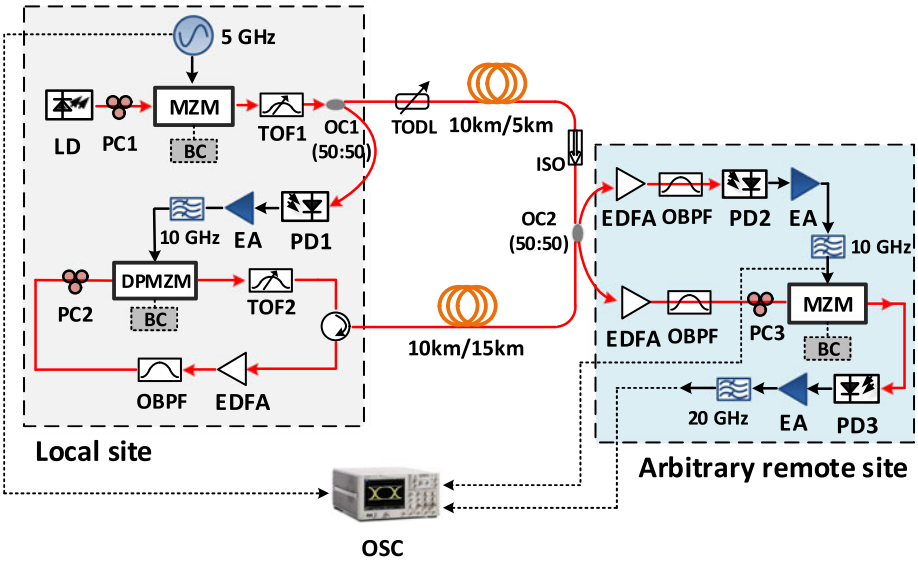

Fig. 2. Experiment setup of the proposed all-optical quadruple frequency dissemination over an arbitrary-point fiber loop link. Two arbitrary remote sites are located between 10 km and 10 km SMF spools, and between 5 km and 15 km SMF spools, respectively. PC: polarization controller. BC: bias control. EA: electronic amplifier. EDFA: erbium-doped fiber amplifier. OBPF: optical bandpass filter. ISO: isolator. OSC: oscilloscope. TODL: tunable optical delay line.

filters a cleared 10-GHz RF signal out. A tunable optical delay line (TODL, General Photonics VDL-001) with tunable range of 330 ps is inserted before the 10-km SMF1 to simulate the fiber-length variation.

At the remote site, two erbium-doped fiber amplifiers (EDFAs) boost the transferred optical signals and maintain the input optical power of the PDs at ~5 dBm. The bandwidths of PD2 and PD3 are 12 GHz and 22 GHz, respectively. The amplified spontaneous emission (ASE) noise derived from the EDFAs is suppressed by optical bandpass filters (OBPFs). MZM3 at the remote site is a 40 Gb/s intensity modulator which is biased at quadrature point. To maintain the three modulators' bias at the desired operation point, the bias control (BC) circuits are applied in the experiment. Moreover, we utilize three polarization controllers (PC1, PC2, and PC3) to control the state of polarization and reduce the polarization-dependence loss. In practice, polarization maintaining optical fibers can be employed to address the polarization problem. A digital sampling oscilloscope (Agilent 86100C) triggered by the 5-GHz standard RF signal is used to record the waveforms and measure the timing delay variation.

Fig. 3(a) and (b) show the optical spectrums at the output of TOF1 and TOF2. We can see that the optical carriers are suppressed by about 18 dB and 28 dB compared with the first-order OSBs, respectively. The high-order OSBs are suppressed below the noise floor by the TOFs, and the ratio of carrier to noise can reach 50 dB and 48 dB. It should be noted that the residual optical carriers may impact the system performance slightly. The residual carrier at the output of TOF2 will superpose with the wanted sidebands, causing the amplitude fluctuation of the received RF signal. Hence, advanced system performance can be completed by using a more balanced modulator and an optical filter with better suppression ratio.

To verify the compensation performance of the proposed scheme intuitively, we first produce a random delay change using the TODL and measure the persistent waveforms of the received signal with the oscilloscope. Fig. 4 shows the recorded waveforms without and with the proposed photonic-microwave-phase-conjugation-based compensation, corresponding to V_3 and V_4 in Fig. 1. As can be seen, without the proposed compensation, the RF signal V_3 at 10 GHz has a large phase jitter caused by adjustment of the TODL. In contrast, the phase fluctuation of the received frequency-quadrupled signal at 20 GHz with compensation is significantly curbed. When the timing delay

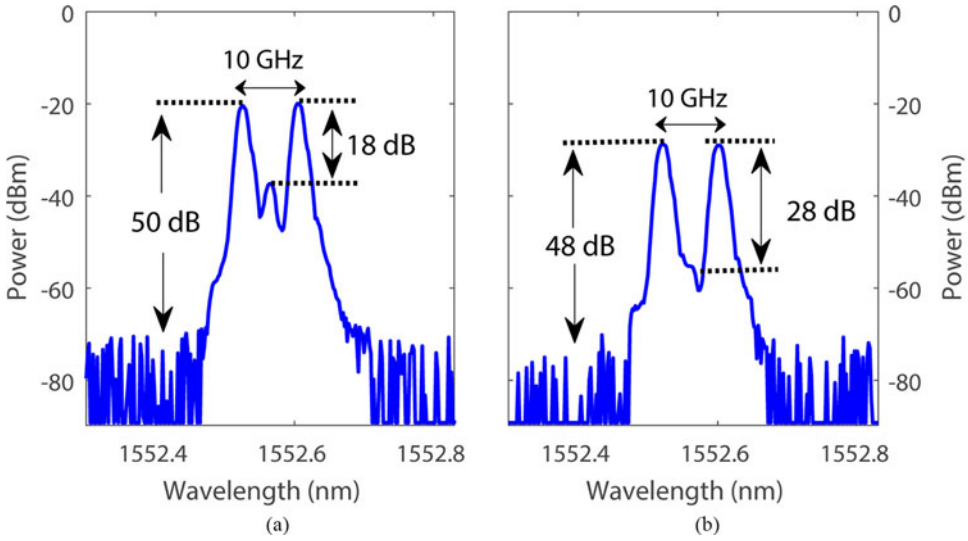

Fig. 3. Optical spectrums at the output of (a) TOF1 and (b) TOF2.

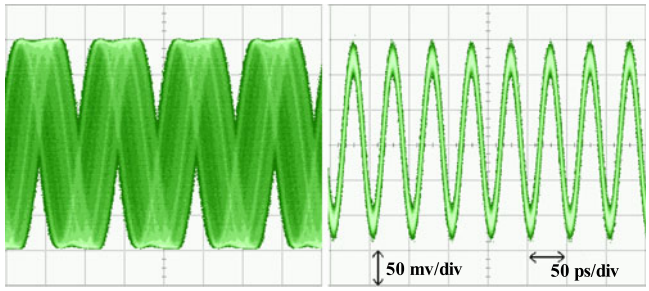

Fig. 4. Persistent waveforms of the RF signal received at the remote site (a) without and (b) with the proposed photonic microwave phase conjugation based compensation by adjustment of the TODL.

is slowly changing with adjustment of the TODL, some amplitude disturbance can be observed in Fig. 4(a) and (b), which is mainly caused by constructive or destructive interference between residual carriers and optical sidebands. In this case, the amplitude fluctuation can be coupled to phase noise at below 1 Hz offset frequency. Furthermore, due to the nonlinearity of MZM3, the amplitude fluctuation in Fig. 4(b) is slightly higher than that in Fig. 4(a).

We also test the stability performance of the scheme under natural changes of the ambient temperature in our laboratory. We carried out the measurement in the evening, and at that time the temperature could randomly fluctuate. Fig. 5(a) shows the measured timing delay variation of the frequency-doubled signal at 10 GHz without compensation and the frequency-quadrupled signal at 20 GHz with compensation in an hour. The timing delay variation without compensation is up to $\sim$180 ps within an hour, which is mainly induced by the ambient temperature change of our laboratory. As a contrast, the delay variation with compensation can be remarkably suppressed to less than $\pm$2 ps, corresponding to an RMS timing jitter of $\sim$0.86 ps. Furthermore, in order to verify the capability of arbitrary-node stable frequency dissemination of this scheme, we also make the measurements at another remote node located between 5 km and 15 km SMF spools. The experimental apparatus of the remote node is just the same as that between 10 km and 10 km SMF spools. The gain of the EDFAs and EAs are adjusted to optimize the signal-to noise ratio of the received signals. The results are shown in Fig. 5(b). For an hour measuring time, the delay variation of the received signal with compensation is likewise stabilized to no more than $\pm$2 ps. This manifests that the scheme supports stable frequency dissemination at an arbitrary remote

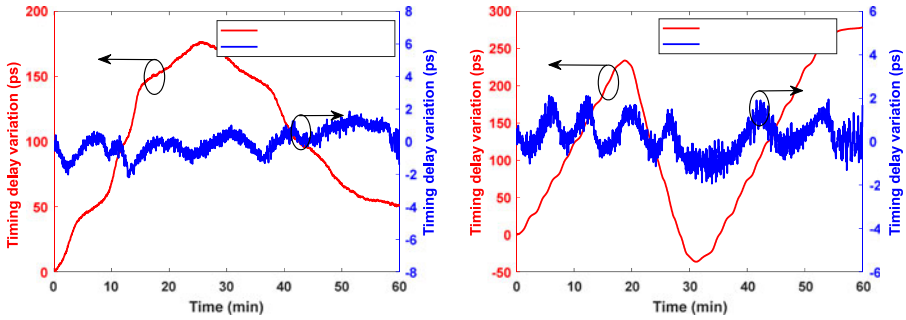

Fig. 5. Measured timing delay variation of the received RF signal at an arbitrary remote site connected by (a) 10km/10km SMF spools and (b) 5 km/15 km SMF spools. (red: the 10 GHz signal without compensation, and blue: the 20 GHz signal with compensation).

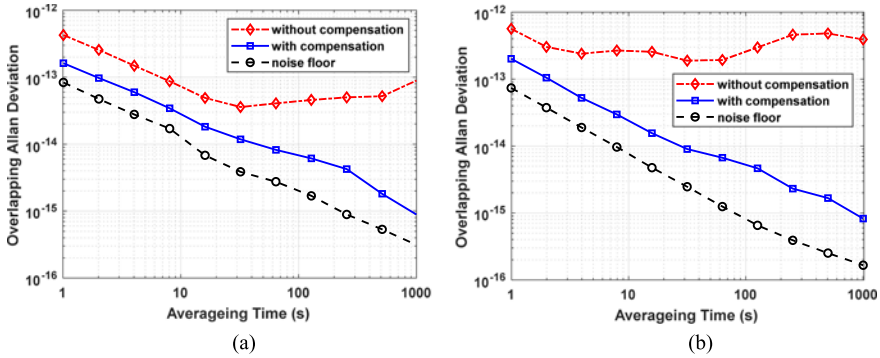

Fig. 6. The overlapping Allan deviation of the proposed frequency dissemination scheme with the remote site located at (a) 10km/10km SMF spools and (b) 5 km/15 km SMF spools. (red: the 10 GHz signal without compensation, blue: the 20 GHz signal with compensation, and black: noise floor).

site. Moreover, in both measurements, a tiny waving delay drift still exists after compensation which is presumably attributed to the slowly changed polarization state of the optical signal induced by polarization mode dispersion (PMD). Further, a polarization scrambler can be inserted to reduce the impact of PMD.

Fig. 6 shows the calculated relative frequency stability based on the time delay variation measurements in Fig. 5, in terms of overlapping Allan deviation (ADEV). Fig. 6(a) and (b) are corresponding to the cases of 10km-10km SMF spools and 5 km-15 km SMF spools, respectively. As shown in Fig. 6(a), the red curve is the result of the 10 GHz RF signal without compensation. Its frequency stability is 4.4×10^{-13} at 1 s, and 9×10^{-14} at 1000 s. After 30 second averaging time, the Allan deviation curve starts increasing, suggesting that the stability of 10-GHz signal without compensation is gradually corrupted due to the lab temperature change. The blue curve is the result of the 20-GHz signal with compensation, which is improved to 1.7×10^{-13} at 1 s, and 8.5×10^{-16} at 1000 s, respectively. Especially at 1000 s averaging time, the relative frequency stability with compensation is two orders of magnitude higher than that without compensation. Fig. 6(b) shows the frequency stability performance at another remote site between 5 km and 15 km SMF spools. The long-term stability with compensation can drop to a value of 8.0×10^{-16} at 1000 s, compared to that of 4.0×10^{-13} at 1000 s without compensation. The fiber delay fluctuation has been also compensated efficiently with the proposed photonic microwave phase conjugation scheme. It can be seen that the frequency stability with compensation is not significantly deteriorated by arbitrarily accessing another remote site. We also measured the noise floor of the compensation system by replacing the 20-km fiber loop link with two 1-m fibers. The results are the black curves in Fig. 6(a) and (b). By comparing the blue and black curves, it can be easily recognized that the trends of

the two curves are similar to each other for both remote sites, which simultaneously validates the effectiveness of the proposed compensation scheme. Nevertheless, the Allan deviation curves with compensation does not reach the same level as the noise floor of the system. It may result from the EDFAs' and EAs' noise which can degrade the phase stability. To mitigate the noise-induced phase stability degradation, phase-sensitive amplifiers and low-noise amplifiers can be used in the experiment [20].

4. Conclusion

In summary, an all-optical stable quadruple frequency dissemination over an arbitrary-point fiber-optic loop link has been proposed and experimentally verified. Here, photonic microwave phase conjugation and photomixing replace the electrical frequency mixing to achieve the phase fluctuation cancellation, thus avoiding the local oscillator leakage and mixing spurs from mixers. A frequency-quadrupled RF signal at 20 GHz can be steadily distributed to any remote site along a 20-km fiber-optic loop link. The residual RMS timing jitter of the stabilized frequency-quadrupled signal within an hour measuring time is no more than 0.86 ps, and long-term frequency stability of 10^{-16} level at 1000 s averaging time can be achieved at an arbitrary remote site. Meanwhile, this scheme combining stable frequency transfer and frequency quadrupling operation is unconstrained by the frequency and bandwidth of the modulator and electrical devices, and can be extended to the field of phase-array millimeter-wave antennas and highly stable millimeter-wave signal distribution.

References

[1] M. Xin *et al.*, "Attosecond precision multi-kilometer laser-microwave network," *Light, Sci. Appl.*, vol. 6, 2017, Art. no. e16187.
[2] J. Kim, J. A. Cox, J. Chen, and F. X. Kartner, "Drift-free femtosecond timing synchronization of remote optical and microwave sources," *Nature Photon.*, vol. 2, pp. 733–736, 2008.
[3] F. Riehle, "Optical clock networks," *Nature Photon.*, vol. 11, pp. 25–31, 2017.
[4] J. Capmany and D. Novak, "Microwave photonics combines two worlds," *Nature Photon.*, vol. 1, pp. 319–330, 2007.
[5] J. Yao, "Microwave photonics," *J. Lightw. Technol.*, vol. 27, pp. 314–335, 2009.
[6] S. W. Schediwy, D. R. Gozzard, S. Stobie, J. A. Malan, and K. Grainge, "Stabilized microwave-frequency transfer using optical phase sensing and actuation," *Opt. Lett.*, vol. 42, pp. 1648–1651, 2017.
[7] L. Sliwczynski and P. Krehlik, "Multipoint joint time and frequency dissemination in delay-stabilized fiber optic links," *IEEE Trans. Ultrason., Ferroelectr., Freq. Control*, vol. 62, no. 3, pp. 412–420, Mar. 2015.
[8] O. Lopez *et al.*, "86-km optical link with a resolution of 2 $\times$ 10–18 for rf frequency transfer," *Eur. Phys. J. D-Atomic, Molecular, Opt. Plasma Phys.*, vol. 48, pp. 35–41, 2008.
[9] A. Zhang *et al.*, "Phase stabilized downlink transmission for wideband radio frequency signal via optical fiber link," *Opt. Exp.*, vol. 22, pp. 21560–21566, 2014.
[10] X. Wang, Z. Liu, S. Wang, D. Sun, Y. Dong, and W. Hu, "Photonic radio-frequency dissemination via optical fiber with high-phase stability," *Opt. Lett.*, vol. 40, pp. 2618–2621, 2015.
[11] W. Li, W. Wang, W. Sun, W. Wang, and N. Zhu, "Stable radio-frequency phase distribution over optical fiber by phase-drift auto-cancellation," *Opt. Lett.*, vol. 39, pp. 4294–4296, 2014.
[12] J. Wei, F. Zhang, Y. Zhou, D. Ben, and S. Pan, "Stable fiber delivery of radio-frequency signal based on passive phase correction," *Opt. Lett.*, vol. 39, pp. 3360–3362, 2014.
[13] Y. B. He *et al.*, "Stable radio-frequency transfer over optical fiber by phase-conjugate frequency mixing," *Opt. Exp.*, vol. 21, pp. 18754–18764, 2013.
[14] K. Y. Lau, G. F. Lutes, and R. L. Tjoelker, "Ultra-stable rf-over-fiber transport in nasa antennas, phased arrays and radars," *J. Lightw. Technol.*, vol. 32, pp. 3440–3451, 2014.
[15] S. Zhang and J. Zhao, "Frequency comb-based multiple-access ultrastable frequency dissemination with 7 $\times$ 10(−17) instability," *Opt. Lett.*, vol. 40, pp. 37–40, 2015.
[16] L. Yu *et al.*, "Wdm-based radio frequency dissemination in a tree-topology fiber optic network," *Opt. Exp.*, vol. 23, pp. 19783–19792, 2015.
[17] H. Li, G. Wu, J. Zhang, J. Shen, and J. Chen, "Multi-access fiber-optic radio frequency transfer with passive phase noise compensation," *Opt. Lett.*, vol. 41, pp. 5672–5675, 2016.
[18] C. Liu *et al.*, "Gvd-insensitive stable radio frequency phase dissemination for arbitrary-access loop link," *Opt. Exp.*, vol. 24, pp. 23376–23382, 2016.
[19] S. Li, X. Zheng, H. Zhang, and B. Zhou, "Compensation of dispersion-induced power fading for highly linear radio-over-fiber link using carrier phase-shifted double sideband modulation," *Opt. Lett.*, vol. 36, no. 4, pp. 546–548, 2011.
[20] S. L. Olsson, H. Eliasson, E. Astra, M. Karlsson, and P. A. Andrekson, "Long-haul optical transmission link using low-noise phase-sensitive amplifiers," *Nature Commun.*, vol. 9, no. 1, 2018, Art. no. 2513.